



Implementing Two Generalizations of the Friis Transmission Formula

FRÉDÉRIC BROYDÉ¹, EVELYNE CLAVELIER², LUKAS JELINEK³,
MILOSLAV CAPEK³ and KARL F. WARNICK⁴

¹Eurexcem, 12 chemin des Hauts de Clairefontaine, 78580 Maule, France

²Excem, 12 chemin des Hauts de Clairefontaine, 78580 Maule, France

³Department of Electromagnetic Field, Czech Technical University in Prague, Technicka 166 27, Czech Republic

⁴Department of Electrical and Computer Engineering, Brigham Young University, Provo, UT 84602, USA

Corresponding author: Frédéric Broydé (e-mail: fredbroyde@eurexcem.com).

ABSTRACT Two generalizations of the Friis transmission formula are based on the concept of unnamed power gain, defined as the ratio of the available power at the port(s) of one or more receiving antennas to the average power received by the port(s) of one or more transmitting antennas. The first generalization is about one transmitting antenna and one receiving antenna, at any distance, in any environment. The second generalization encompasses the first one. It is about two multiport antenna arrays, one used for emission and the other for reception, at any distance, in any environment. Both generalizations say that the unnamed power gains have two properties, referred to as “symmetry under link direction reversal” and “vanishing sensitivity to terminations for small coupling”. The definitions of these properties for multiport antenna arrays are somewhat more involved than the ones applicable to the two-antenna case. We implement these generalizations in numerical experiments comprising two or six antennas, to observe and analyze the behavior of the unnamed power gains and these properties. We also define and investigate a new concept: the rank measure of the unnamed power gain.

INDEX TERMS Antenna theory, Friis transmission formula, MIMO, antenna array, reciprocity.

I. INTRODUCTION

In 1946, Friis proposed a transmission formula concerning “a radio circuit made up of a transmitting antenna and a receiving antenna in free space”. It became a cornerstone of antenna and radio communication engineering, and was therefore adapted into different forms to meet varying needs. The original Friis transmission formula is [1]:

$$\frac{P_{avr}}{P_t} = \frac{A_r A_t}{d^2 \lambda^2}, \quad (1)$$

in which: P_{avr} is the average power available at the port of the receiving antenna; P_t is the average power fed into the transmitting antenna at its port; A_r is the effective area of the receiving antenna, in the direction of the transmitting antenna; A_t is the effective area of the transmitting antenna, in the direction of the receiving antenna; d is a distance between the antennas; and λ is the wavelength of the sinusoidal signal delivered to the transmitting antenna.

The applicable definition of the average power available at the port of the receiving antenna, also referred to as “available power” at this port, is the greatest average power that can be drawn from this port by an arbitrary linear time-invariant

(LTI) and passive load [2, Sec. 3-8], [3]. The applicable definition of the effective area of an antenna in a given direction is: “the ratio of the available power at the terminals of a receiving antenna to the power flux density of a plane wave incident on the antenna from that direction, the wave being polarization matched to the antenna” [4].

The Friis transmission formula (1) is about two single-port antennas. It assumes that they are polarization matched, that d is sufficiently large (far-field condition), and that the transmitting antenna is reciprocal. Here, “reciprocal antenna” means an antenna to which we could apply the Lorentz reciprocity theorem if it was used in free space [5, Sec. 13.1].

For polarization-matched antennas and sufficiently large values of d , another form of (1) is [5, Sec. 4.4.2], [6]:

$$\frac{P_{avr}}{P_t} = \frac{A_r G_t}{4\pi d^2}, \quad (2)$$

where G_t is the gain of the transmitting antenna, in the direction of the receiving antenna. The gain of an antenna in a given direction being defined as “the ratio of the radiation intensity in a given direction to the radiation intensity that would be produced if the power accepted by the antenna

were isotropically radiated” [4], (2) directly follows from the definitions of A_r and G_t , and therefore does not require any assumption on the reciprocity of the transmitting antenna.

Another common form of (1) for polarization-matched antennas and sufficiently large values of d is [5, Sec. 4.4.2]:

$$\frac{P_{avr}}{P_t} = G_r G_t \left(\frac{\lambda}{4\pi d} \right)^2, \quad (3)$$

where G_r is the gain of the receiving antenna, in the direction of the transmitting antenna. This formula applies only to a reciprocal receiving antenna.

A ratio of the available power at the port(s) of one or more receiving antennas to the average power received by the port(s) of one or more transmitting antennas is an unnamed power gain [7, Sec. IV], [8, Sec. IX]. Thus, (1)–(3) are about the unnamed power gain of a radio link. Moreover, a teaching of (1) and (3) is that, if, without moving the antennas, their roles are reversed (i.e., the receiving antenna becomes the transmitting antenna and vice versa), then the unnamed power gains in the two configurations are equal, if they are defined and if both antennas are reciprocal.

In [7, Sec. VII], a first generalization of the Friis transmission formula was proposed. This first generalization is also about one transmitting antenna and one receiving antenna, but it neither assumes polarization-matched antennas, nor a large value of d , nor a free space environment. As explained in Section II, it says that the unnamed power gains between the antennas have two important properties: the “symmetry under link direction reversal” and the “vanishing sensitivity to terminations for small coupling”.

Numerical experiments involving simple two-antenna setups are used in Section III to study the first generalization, in free space or in a half-space bounded by a ground plane. The behaviors of the unnamed power gain and other power gains are compared in Section III.

In [8, Sec. XIII], a second generalization of the Friis transmission formula was proposed, in which a multiport antenna array (MAA) coupled to a multiport generator is used for emission and a MAA coupled to a multiport load is used for reception. In this context, the unnamed power gain depends on the excitation. Like the first one, the second generalization neither assumes a large value of the distance between the MAAs, nor a free space environment, nor any form of polarization-matching. As explained in Section IV, it says that the unnamed power gains between the MAAs have two important properties, referred to as “symmetry under link direction reversal” and “vanishing sensitivity to terminations for small coupling”, as in the two-antenna case but according to more general definitions. In Section V, we define two new parameters called the rank measures of the unnamed power gain, and we prove a fundamental theorem about them.

Numerical experiments involving simple six-antenna setups are used in Section VI to study the second generalization and the rank measures of the unnamed power gain, in free space or in a half-space bounded by a ground plane.

Corrections to known errors in [7] and [8] are provided in Appendix A.

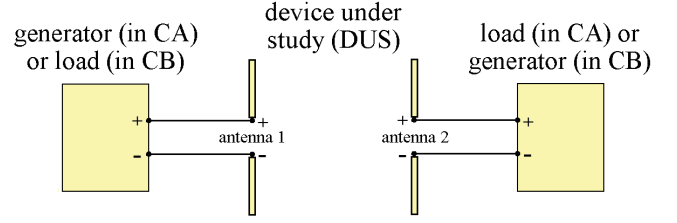


FIGURE 1. The configurations considered in Section II, in which the DUS comprises antenna 1, antenna 2 and their surroundings.

II. THE FIRST GENERALIZATION OF THE FRIIS TRANSMISSION FORMULA

In this Section II, we consider two LTI and passive antennas operating in the harmonic steady state, at a given frequency. We assume that the medium surrounding the antennas is LTI (and passive), so that the antennas in this medium form a passive LTI 2-port referred to as “device under study” (DUS), port 1 of DUS being the port of antenna 1, and port 2 of DUS being the port of antenna 2. For simplicity and brevity, we assume that the DUS has an impedance matrix denoted by \mathbf{Z} , though this assumption was not needed in [7].

The antennas are used in two configurations, which are shown in Fig. 1. In configuration A (CA), antenna 1 is used for emission and antenna 2 for reception, port 1 of the DUS being connected to an LTI generator of internal impedance Z_{S1} , and port 2 of the DUS being connected to an LTI load of impedance Z_{S2} . In configuration B (CB), antenna 2 is used for emission and antenna 1 for reception, port 1 of the DUS being connected to an LTI load of impedance Z_{S1} , and port 2 of the DUS being connected to an LTI generator of internal impedance Z_{S2} . Using $\text{Re}(z)$ to denote the real part of a complex number z , we assume that $\text{Re}(Z_{S1}) > 0$ and $\text{Re}(Z_{S2}) > 0$. This ensures that the loads are passive. We define the matrix

$$\mathbf{Z}_{ADD} = \begin{pmatrix} Z_{S1} & 0 \\ 0 & Z_{S2} \end{pmatrix}. \quad (4)$$

As explained in [7, Sec. II.B], the matrix $\mathbf{Z} + \mathbf{Z}_{ADD}$ is invertible, so that we can define the matrix

$$\mathbf{Y}_{SAM} = \begin{pmatrix} Y_{SAM11} & Y_{SAM12} \\ Y_{SAM21} & Y_{SAM22} \end{pmatrix} = (\mathbf{Z} + \mathbf{Z}_{ADD})^{-1}, \quad (5)$$

\mathbf{Y}_{SAM} being symmetric if and only if \mathbf{Z} is symmetric.

We use G_{AU} to denote the unnamed power gain in CA, and G_{BU} to denote the unnamed power gain in CB. To ensure that they are both defined for any nonzero excitation, we assume that $Y_{SAM11} \neq 0$, $\text{Re}(Y_{SAM11}^{-1} - Z_{S1}) \neq 0$, $Y_{SAM22} \neq 0$ and $\text{Re}(Y_{SAM22}^{-1} - Z_{S2}) \neq 0$, and we obtain [7]:

$$G_{AU} = \frac{Y_{AAVP2}}{Y_{ARP1}}, \quad (6)$$

and

$$G_{BU} = \frac{Y_{BAVP1}}{Y_{BRP2}}, \quad (7)$$

where

$$Y_{AAVP2} = \frac{|Y_{SAM21}|^2}{4\text{Re}(Y_{SAM22} - |Y_{SAM22}|^2 Z_{S2})}, \quad (8)$$

$$Y_{ARP1} = \text{Re} (Y_{SAM11} - |Y_{SAM11}|^2 Z_{S1}) , \quad (9)$$

$$Y_{BAVP1} = \frac{|Y_{SAM12}|^2}{4\text{Re} (Y_{SAM11} - |Y_{SAM11}|^2 Z_{S1})} , \quad (10)$$

and

$$Y_{BRP2} = \text{Re} (Y_{SAM22} - |Y_{SAM22}|^2 Z_{S2}) . \quad (11)$$

More results about Y_{AAVP2} , Y_{ARP1} , Y_{BAVP1} and Y_{BRP2} are provided in Appendix B.

We now assume that both antennas are reciprocal and that the medium surrounding them is reciprocal [9, Sec. 13.06]. By theorem II of [10], known as the ‘‘Rayleigh-Carson reciprocity theorem’’ and corresponding to [9, eq. (13-40)], \mathbf{Z} is symmetric, so that \mathbf{Y}_{SAM} is symmetric, that is to say $Y_{SAM21} = Y_{SAM12}$. Using (6)–(11), we get

$$G_{AU} = G_{BU} \quad (12)$$

for any nonzero excitation. We call this property ‘‘symmetry under link direction reversal’’. It means that, if the stated conditions are satisfied, the unnamed power gain does not change when the direction of the link is reversed.

The unnamed power gain has another important property [7, Sec. VII]: for nonzero excitations, if said conditions are satisfied and the distance D between the antennas is such that the interaction between them is small, $G_{AU} = G_{BU}$ depends very little on Z_{S1} and very little on Z_{S2} . We refer to this result as the ‘‘vanishing sensitivity to terminations for small coupling’’.

The symmetry under link direction reversal and the vanishing sensitivity to terminations for small coupling form the first generalization of the Friis transmission formula.

III. SOME TWO-ANTENNA SETUPS

A. TWO PARALLEL ANTENNAS IN FREE SPACE

We consider an arrangement of two perfectly conducting parallel center-fed cylindrical dipole antennas lying in free space, shown in the not-to-scale drawing of Fig. 2. We use λ to denote the wavelength. The total length of antenna 1 is $l_1 = 0.94 \lambda/2$. The total length of antenna 2 is $l_2 = 0.94 \lambda/4$. Both antennas have the same wire diameter $l_1/50$.

Four setups are defined as follows:

- in setup ‘‘a’’, we assume that $Z_{S1} = 73 \Omega$ and that $Z_{S2} = (1 + j20) \Omega$;
- in setup ‘‘b’’, we assume that $Z_{S1} = (0.05 - j16) \Omega$ and that $Z_{S2} = (10 + j270) \Omega$;
- in setup ‘‘c’’, we assume that $Z_{S1} = (10 + j10) \Omega$ and that $Z_{S2} = (10 + j270) \Omega$; and
- in setup ‘‘d’’, we assume that $Z_{S1} = (0.05 - j16) \Omega$ and that $Z_{S2} = (1 + j20) \Omega$.

We have computed $G_{AU} = G_{BU}$ as a function of D , using (6)–(11) and the simulation technique summarized in Appendix C. Fig. 3 shows $G_{AU} = G_{BU}$ for the different setups. According to the vanishing sensitivity to terminations for small coupling, we expect the four curves of Fig. 3 to almost merge at a sufficient distance, and this is observed for

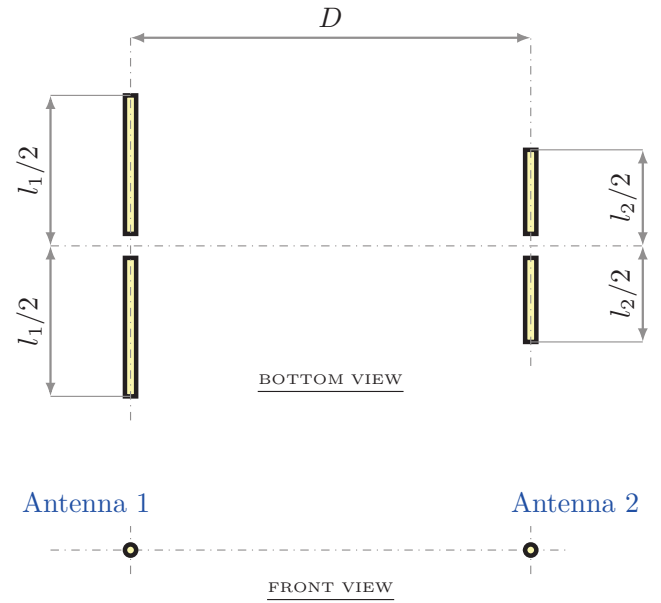


FIGURE 2. An arrangement of two parallel antennas in free space.

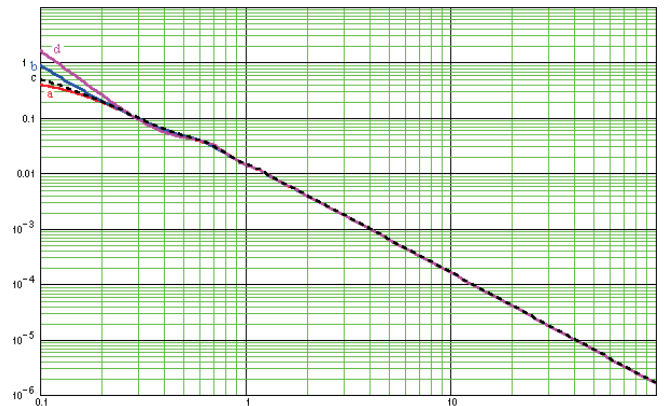


FIGURE 3. Unnamed power gains for the four different setups defined for the arrangement of Fig. 2, as a function of D/λ .

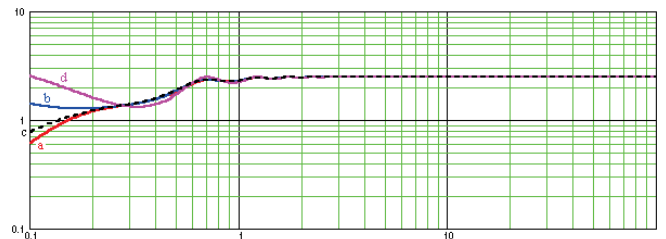


FIGURE 4. Parameter g_T for the four different setups defined for the arrangement of Fig. 2, as a function of D/λ .

$D \geq 0.6 \lambda$. For setup ‘‘d’’, we note that $G_{AU} = G_{BU} > 1$ at very short distances, and $G_{AU} = G_{BU} \simeq 1.6$ at $D = 0.1 \lambda$.

Fig. 4 shows the parameter

$$g_T = \left(\frac{4\pi d}{\lambda} \right)^2 G_{AU} = \left(\frac{4\pi d}{\lambda} \right)^2 G_{BU} . \quad (13)$$

The plateau of g_T indicates that, in each setup, the Friis transmission formula (1)–(3) gives an accurate value of $G_{AU} = G_{BU}$ if $D \geq 1.5 \lambda$, and that $G_r G_t \simeq 2.5$ in (3).

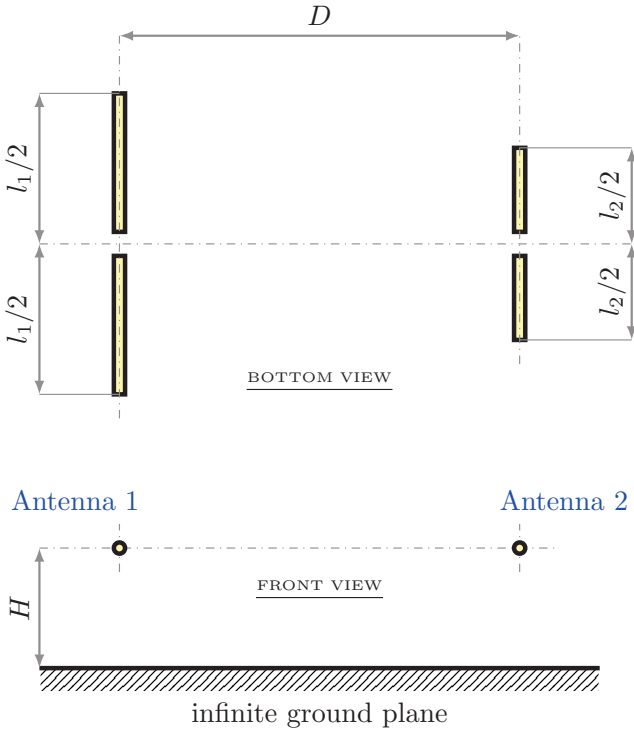


FIGURE 5. Two parallel antennas above a ground plane.

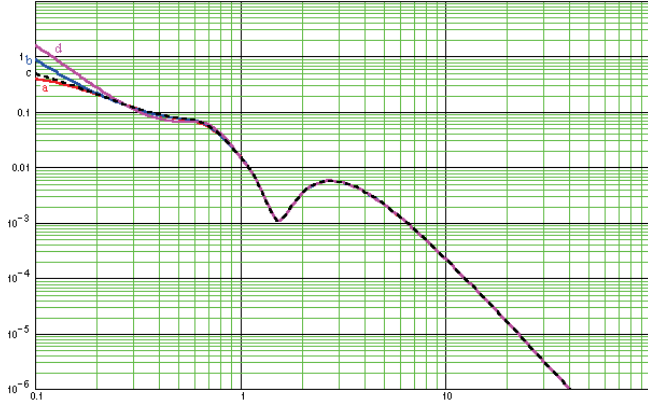


FIGURE 6. Unnamed power gains for the four different setups defined for the arrangement of Fig. 5 and $H = \lambda$, as a function of D/λ .

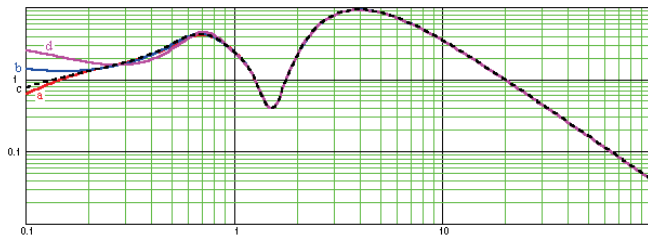


FIGURE 7. Parameter g_T for four different setups defined for the arrangement of Fig. 5 and $H = \lambda$, as a function of D/λ .

B. PARALLEL ANTENNAS ABOVE A GROUND PLANE

We now look at an arrangement of two perfectly conducting parallel center-fed cylindrical dipole antennas lying parallel to an infinite and perfectly conducting ground plane, shown

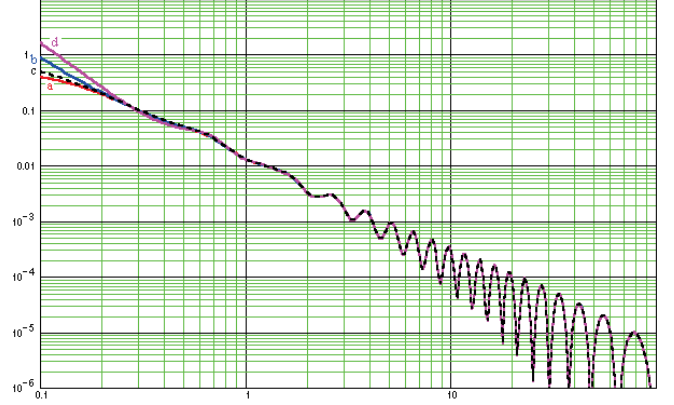


FIGURE 8. Unnamed power gains for the four different setups defined for the arrangement of Fig. 5 and $H = 10\lambda$, as a function of D/λ .

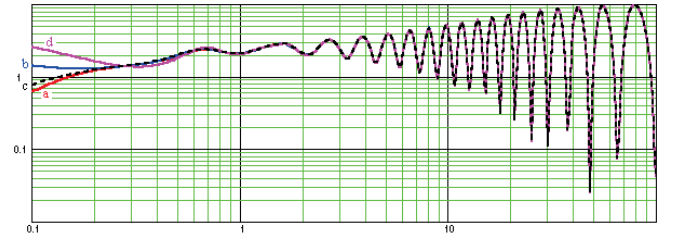


FIGURE 9. Parameter g_T for four different setups defined for the arrangement of Fig. 5 and $H = 10\lambda$, as a function of D/λ .

in the not-to-scale drawing of Fig. 5. The antennas are identical to the one used in Fig. 2. We use H to denote the height of both antennas above the ground plane. Four different setups are defined as above for Fig. 2.

$G_{AU} = G_{BU}$ was computed as above in Section III.A. Fig. 6 and Fig. 7 show $G_{AU} = G_{BU}$ and g_T for $H = \lambda$. Fig. 8 and Fig. 9 show $G_{AU} = G_{BU}$ and g_T for $H = 10\lambda$. In Fig. 6 to Fig. 9, the four curves practically merge in the region $D \geq 0.6\lambda$, in line with the vanishing sensitivity to terminations for small coupling. In the case of setup “d”, Fig. 6 and Fig. 8 show that $G_{AU} = G_{BU}$ is again greater than 1 at very short distances. Clearly, (3) cannot be used in setups involving a ground plane.

C. RESULTS ABOUT OTHER POWER GAINS

In addition to the unnamed power gain, four other power gains were investigated in [7]: the insertion power gain, the transducer power gain, the operating power gain and the available power gain. For nonzero excitations, if the distance D between the antennas is such that the interaction between them is small, simulations showed that none of these other power gains, in CA or in CB, is such that it depends very little on Z_{S1} and very little on Z_{S2} . This was observed in setups using the free-space arrangement of Fig. 2, and the half-space arrangement of Fig. 5.

D. TEACHING OF THE NUMERICAL EXPERIMENTS

Our 2-antenna numerical experiments exemplify the vanishing sensitivity to terminations for small coupling, and show that this property is unique to the unnamed power gain.

IV. THE SECOND GENERALIZATION OF THE FRIIS TRANSMISSION FORMULA

In this Section IV, we consider two LTI and passive MAAs operating in the harmonic steady state, at a given frequency, MAA 1 having m ports numbered from 1 to m , and MAA 2 having n ports numbered from 1 to n , where m and n are positive integers. We assume that the medium surrounding the MAAs is LTI and passive. Thus, the MAAs in this medium form a passive LTI multiport referred to as “device under study” (DUS) and having 2 sets of ports, called port set 1 and port set 2. Port set 1 consists of the m ports of MAA 1, and port set 2 consists of the n ports of MAA 2. The $m + n$ ports of the DUS are considered in the following order: ports 1 to m of port set 1, then ports 1 to n of port set 2. For simplicity and brevity, we assume that the DUS has an impedance matrix denoted by \mathbf{Z} , though this assumption was not needed in [8]. The matrix \mathbf{Z} is of size $m + n$ by $m + n$.

The MAAs are used in two configurations, which are shown in Fig. 10. In configuration A (CA), MAA 1 is used for emission and MAA 2 for reception, port set 1 being connected to an LTI m -port generator of internal impedance matrix \mathbf{Z}_{S1} , and port set 2 being connected to an LTI n -port load of impedance matrix \mathbf{Z}_{S2} . In configuration B (CB), MAA 2 is used for emission and MAA 1 for reception, port set 1 being connected to an LTI m -port load of impedance matrix \mathbf{Z}_{S1} , and port set 2 being connected to an LTI n -port generator of internal impedance matrix \mathbf{Z}_{S2} .

Let \mathbf{M} be a complex matrix. We use \mathbf{M}^* to denote the hermitian adjoint of \mathbf{M} . If \mathbf{M} is square, $\text{tr } \mathbf{M}$ denotes the trace of \mathbf{M} and $H(\mathbf{M})$ denotes the hermitian part of \mathbf{M} , that is to say $(\mathbf{M} + \mathbf{M}^*)/2$. We assume that $H(\mathbf{Z}_{S1})$ and $H(\mathbf{Z}_{S2})$ are positive definite. This ensures that the loads are passive. We define the matrix

$$\mathbf{Z}_{ADD} = \begin{pmatrix} \mathbf{Z}_{S1} & \mathbf{0} \\ \mathbf{0} & \mathbf{Z}_{S2} \end{pmatrix}. \quad (14)$$

As explained in [11, Sec. II], the matrix $\mathbf{Z} + \mathbf{Z}_{ADD}$ is invertible, so that we can define the matrix

$$\mathbf{Y}_{SAM} = (\mathbf{Z} + \mathbf{Z}_{ADD})^{-1}, \quad (15)$$

and, if \mathbf{Z}_{ADD} is symmetric, \mathbf{Y}_{SAM} is symmetric if and only if \mathbf{Z} is symmetric. The matrix \mathbf{Y}_{SAM} is of size $(m + n)$ by $(m + n)$ and it may be partitioned into four submatrices, \mathbf{Y}_{SAM11} of size m by m , \mathbf{Y}_{SAM12} of size m by n , \mathbf{Y}_{SAM21} of size n by m and \mathbf{Y}_{SAM22} of size n by n , which are such that

$$\mathbf{Y}_{SAM} = \begin{pmatrix} \mathbf{Y}_{SAM11} & \mathbf{Y}_{SAM12} \\ \mathbf{Y}_{SAM21} & \mathbf{Y}_{SAM22} \end{pmatrix}. \quad (16)$$

As in Section II, we use G_{AU} to denote the unnamed power gain in CA, and G_{BU} to denote the unnamed power gain in CB. To ensure that they are both defined for any nonzero excitation, we assume that \mathbf{Y}_{SAM11} , \mathbf{Y}_{SAM22} , $H(\mathbf{Y}_{SAM11}^{-1} - \mathbf{Z}_{S1})$ and $H(\mathbf{Y}_{SAM22}^{-1} - \mathbf{Z}_{S2})$ are invertible.

Following [8], we define the positive definite matrices

$$\mathbf{Y}_{AAVP2} = \frac{1}{4} \mathbf{Y}_{SAM21}^* \mathbf{Y}_{SAM22}^{-1*} \times H(\mathbf{Y}_{SAM22}^{-1} - \mathbf{Z}_{S2})^{-1} \mathbf{Y}_{SAM22}^{-1} \mathbf{Y}_{SAM21}, \quad (17)$$

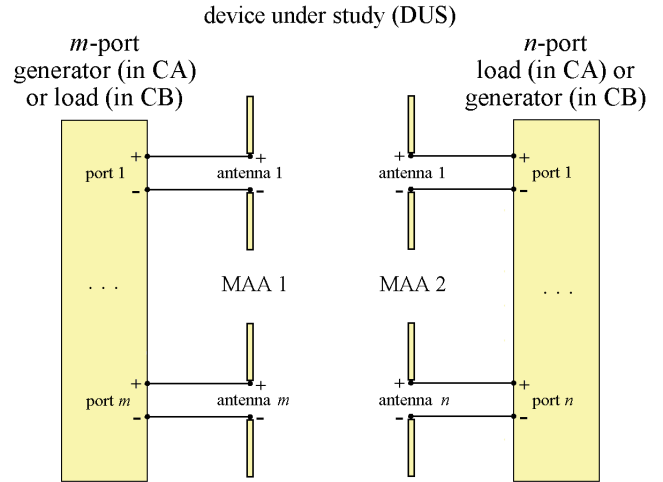


FIGURE 10. The two configurations considered in Section IV, in which the DUS comprises MAA 1, MAA 2 and their surroundings.

$$\mathbf{Y}_{ARP1} = \mathbf{Y}_{SAM11}^* H(\mathbf{Y}_{SAM11}^{-1} - \mathbf{Z}_{S1}) \mathbf{Y}_{SAM11}, \quad (18)$$

$$\mathbf{Y}_{BAVP1} = \frac{1}{4} \mathbf{Y}_{SAM12}^* \mathbf{Y}_{SAM11}^{-1*} \times H(\mathbf{Y}_{SAM11}^{-1} - \mathbf{Z}_{S1})^{-1} \mathbf{Y}_{SAM11}^{-1} \mathbf{Y}_{SAM12}, \quad (19)$$

and

$$\mathbf{Y}_{BRP2} = \mathbf{Y}_{SAM22}^* H(\mathbf{Y}_{SAM22}^{-1} - \mathbf{Z}_{S2}) \mathbf{Y}_{SAM22}. \quad (20)$$

Other results about \mathbf{Y}_{AAVP2} , \mathbf{Y}_{ARP1} , \mathbf{Y}_{BAVP1} and \mathbf{Y}_{BRP2} are provided in Appendix D. We have

$$G_{AU} = \frac{\mathbf{V}_{O1}^* \mathbf{Y}_{AAVP2} \mathbf{V}_{O1}}{\mathbf{V}_{O1}^* \mathbf{Y}_{ARP1} \mathbf{V}_{O1}} \quad (21)$$

and

$$G_{BU} = \frac{\mathbf{V}_{O2}^* \mathbf{Y}_{BAVP1} \mathbf{V}_{O2}}{\mathbf{V}_{O2}^* \mathbf{Y}_{BRP2} \mathbf{V}_{O2}}, \quad (22)$$

where \mathbf{V}_{O1} and \mathbf{V}_{O2} are the column vectors of the rms open-circuit voltages of the m -port generator connected to port set 1 in CA, and of the n -port generator connected to port set 2 in CB, respectively. Accordingly, G_{AU} and G_{BU} depend on the excitation. This dependence is immaterial for G_{AU} if $m = 1$, and for G_{BU} if $n = 1$.

It is shown in [8, Sec. IX] that:

- the set of the values of the unnamed power gain in CA, obtained for all nonzero excitations, has a least element referred to as “minimum value” and denoted by G_{AUMIN} , and a greatest element referred to as “maximum value” and denoted by G_{AUMAX} ;
- the eigenvalues of the matrix

$$\mathbf{T}_{AU} = \mathbf{Y}_{AAVP2} \mathbf{Y}_{ARP1}^{-1} \quad (23)$$

are real, G_{AUMIN} being the smallest eigenvalue of \mathbf{T}_{AU} and G_{AUMAX} the largest eigenvalue of \mathbf{T}_{AU} ;

- an average value of G_{AU} over a number $\min\{m, n\}$ of nonzero excitations is

$$G_{AUAVR} = \frac{\text{tr } \mathbf{T}_{AU}}{\min\{m, n\}}; \quad (24)$$

- (d) the set of the values of the unnamed power gain in CB, obtained for all nonzero excitations, has a least element referred to as “minimum value” and denoted by $G_{BU\ MIN}$, and a greatest element referred to as “maximum value” and denoted by $G_{BU\ MAX}$;
- (e) the eigenvalues of the matrix

$$\mathbf{T}_{BU} = \mathbf{Y}_{BAVP1} \mathbf{Y}_{BRP2}^{-1} \quad (25)$$

- are real, $G_{BU\ MIN}$ being the smallest eigenvalue of \mathbf{T}_{BU} and $G_{BU\ MAX}$ the largest eigenvalue of \mathbf{T}_{BU} ; and
- (f) an average value of G_{BU} over a number $\min\{m, n\}$ of nonzero excitations is

$$G_{BU\ AVR} = \frac{\text{tr } \mathbf{T}_{BU}}{\min\{m, n\}}. \quad (26)$$

We now assume that both MAAs and the medium surrounding them are reciprocal. It follows from the Rayleigh-Carson reciprocity theorem that \mathbf{Z} is symmetric. We also posit that \mathbf{Z}_{S1} and \mathbf{Z}_{S2} are symmetric, so that \mathbf{Y}_{SAM} is symmetric. It is shown in [8, Sec. IX] that

$$G_{AU\ MAX} = G_{BU\ MAX}, \quad (27)$$

$$G_{AU\ AVR} = G_{BU\ AVR}, \quad (28)$$

$$(m = n) \implies (G_{AU\ MIN} = G_{BU\ MIN}), \quad (29)$$

$$(m > n) \implies (G_{AU\ MIN} = 0) \quad (30)$$

and

$$(m < n) \implies (G_{BU\ MIN} = 0). \quad (31)$$

We call (27)–(31) “symmetry under link direction reversal”. It means that, if the stated conditions are satisfied, the maximum value of the unnamed power gain for all nonzero excitations, the minimum value of the unnamed power gain for all nonzero excitations, and the average value of the unnamed power gain do not change when the direction of the radio link is reversed.

The unnamed power gain between two MAAs has another fundamental property. It says that, if said conditions are satisfied and the distance D between the MAAs is such that the interaction between them is small, then [8, Sec. XIII]: $G_{AU\ MAX} = G_{BU\ MAX}$ and $G_{AU\ AVR} = G_{BU\ AVR}$ depend very little on \mathbf{Z}_{S1} and \mathbf{Z}_{S2} ; and, if $m = n$, then $G_{AU\ MIN} = G_{BU\ MIN}$ depends very little on \mathbf{Z}_{S1} and \mathbf{Z}_{S2} . We refer to this result as the “vanishing sensitivity to terminations for small coupling”, because it generalizes the vanishing sensitivity to terminations for small coupling defined in Section II for two antennas.

The symmetry under link direction reversal and the vanishing sensitivity to terminations for small coupling, applied to two MAAs, form the second generalization of the Friis transmission formula. In the special case $m = n = 1$, it uses the same assumptions and provides the same conclusions as the first generalization studied in Section II.

V. THE RANK MEASURES

To better characterize the radio link shown in Fig. 10 as regards spatial multiplexing or spatial diversity, we propose two new quantities: the rank measure of the unnamed power gain in CA, denoted by ρ_A , and the rank measure of the unnamed power gain in CB, denoted by ρ_B . Their definitions are based on the effective rank of a matrix [12].

We use $\text{rank } \mathbf{M}$ to denote the rank of a complex matrix \mathbf{M} . If \mathbf{M} is of size M by M , such that $\text{rank } \mathbf{M} > 0$, and of singular values $\sigma_1, \dots, \sigma_M$, we define

$$p_k = \frac{\sigma_k}{\sum_{k=1}^M |\sigma_k|} \quad (32)$$

for any $k \in \{1, \dots, M\}$, and the effective rank of \mathbf{M} is given by [12]:

$$\text{erank } \mathbf{M} = \exp \left(- \sum_{k=1}^M p_k \ln p_k \right), \quad (33)$$

where, by convention, $0 \ln 0 = 0$. According to [12], we have:

$$1 \leq \text{erank } \mathbf{M} \leq \text{rank } \mathbf{M} \leq M, \quad (34)$$

where $\text{erank } \mathbf{M} = 1$ if and only if \mathbf{M} has a single nonzero singular value, and where $\text{erank } \mathbf{M} = \text{rank } \mathbf{M}$ if and only if all nonzero singular values of \mathbf{M} are equal.

Moreover, it follows from [13, Sec. 2.6.4] that the effective rank is a continuous function of the entries of \mathbf{M} .

We use $\mathbf{A}^{-1/2}$ to denote the inverse of the unique positive definite square root of a positive definite matrix \mathbf{A} . We posit

$$\rho_A = \text{erank} \left(\mathbf{Y}_{ARP1}^{-1/2} \mathbf{Y}_{AAVP2} \mathbf{Y}_{ARP1}^{-1/2} \right) \quad (35)$$

and

$$\rho_B = \text{erank} \left(\mathbf{Y}_{BRP2}^{-1/2} \mathbf{Y}_{BAVP1} \mathbf{Y}_{BRP2}^{-1/2} \right). \quad (36)$$

Theorem. We assert that:

- the singular values of $\mathbf{Y}_{ARP1}^{-1/2} \mathbf{Y}_{AAVP2} \mathbf{Y}_{ARP1}^{-1/2}$, counting multiplicity, are the eigenvalues of \mathbf{T}_{AU} , counting multiplicity;
- the singular values of $\mathbf{Y}_{BRP2}^{-1/2} \mathbf{Y}_{BAVP1} \mathbf{Y}_{BRP2}^{-1/2}$, counting multiplicity, are the eigenvalues of \mathbf{T}_{BU} , counting multiplicity; and
- if both MAAs and the medium surrounding them are reciprocal, and if \mathbf{Z}_{S1} and \mathbf{Z}_{S2} are symmetric, then

$$\rho_A = \rho_B. \quad (37)$$

Proof: $\mathbf{K}_{AU} = \mathbf{Y}_{ARP1}^{-1/2} \mathbf{Y}_{AAVP2} \mathbf{Y}_{ARP1}^{-1/2}$ is hermitian and similar to \mathbf{T}_{AU} . It follows that \mathbf{K}_{AU} is positive semidefinite. By [14, Sec. 7.3.5], it follows that the singular values of \mathbf{K}_{AU} , counting multiplicity, are the eigenvalues of \mathbf{K}_{AU} , counting multiplicity. Thus (result A), the singular values of \mathbf{K}_{AU} , counting multiplicity, are the eigenvalues of \mathbf{T}_{AU} , counting multiplicity.

Likewise, $\mathbf{K}_{BU} = \mathbf{Y}_{BRP2}^{-1/2} \mathbf{Y}_{BAVP1} \mathbf{Y}_{BRP2}^{-1/2}$ is hermitian and similar to \mathbf{T}_{BU} . Thus (result B), the singular values of

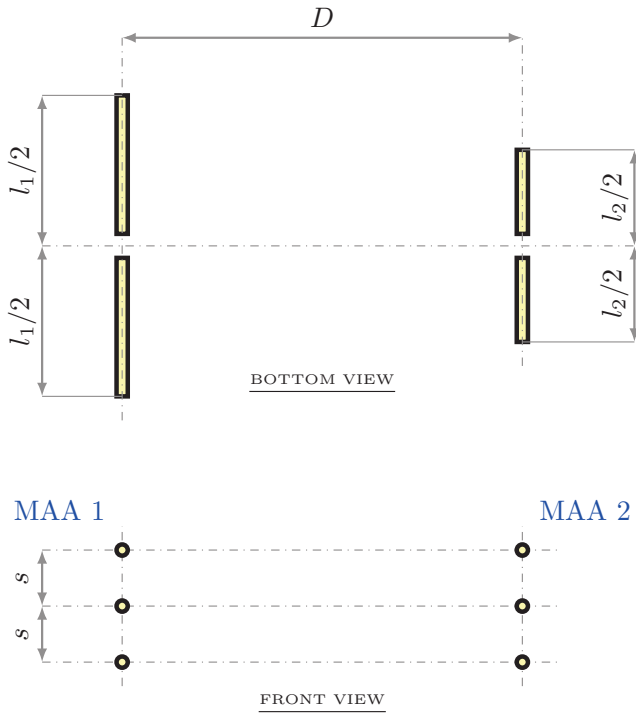


FIGURE 11. An arrangement of six parallel antennas in free space.

\mathbf{K}_{BU} , counting multiplicity, are the eigenvalues of \mathbf{T}_{BU} , counting multiplicity.

If both MAAs and the medium surrounding them are reciprocal, and if \mathbf{Z}_{S1} and \mathbf{Z}_{S2} are symmetric, we have already seen that \mathbf{Y}_{SAM} is symmetric. It follows from the last steps of the proof of Theorem 29 of [8] that (result C):

- if $m = n$, then \mathbf{T}_{AU} and \mathbf{T}_{BU} have the same eigenvalues, counting multiplicity;
- if $m > n$, then \mathbf{T}_{AU} has the same eigenvalues as \mathbf{T}_{BU} , counting multiplicity, together with $m - n$ additional eigenvalues equal to zero; and
- if $m < n$, then \mathbf{T}_{BU} has the same eigenvalues as \mathbf{T}_{AU} , counting multiplicity, together with $n - m$ additional eigenvalues equal to zero.

Using result A, result B and result C, we obtain:

- if $m = n$, then \mathbf{K}_{AU} and \mathbf{K}_{BU} have the same singular values, counting multiplicity;
- if $m > n$, then \mathbf{K}_{AU} has the same singular values as \mathbf{K}_{BU} , counting multiplicity, together with $m - n$ additional singular values equal to zero; and
- if $m < n$, then \mathbf{K}_{BU} has the same singular values as \mathbf{K}_{AU} , counting multiplicity, together with $n - m$ additional singular values equal to zero.

This and (35)–(36) lead us to the last assertion of the theorem. \square

We see that: $\rho_A = m$ if and only if $G_{AU MAX}$ and $G_{AU MIN}$ are equal; and $\rho_A = 1$ if and only if \mathbf{T}_{AU} has a single nonzero eigenvalue.

Likewise, we see that: $\rho_B = n$ if and only if $G_{BU MAX}$ and $G_{BU MIN}$ are equal; and $\rho_B = 1$ if and only if \mathbf{T}_{BU} has a single nonzero eigenvalue.

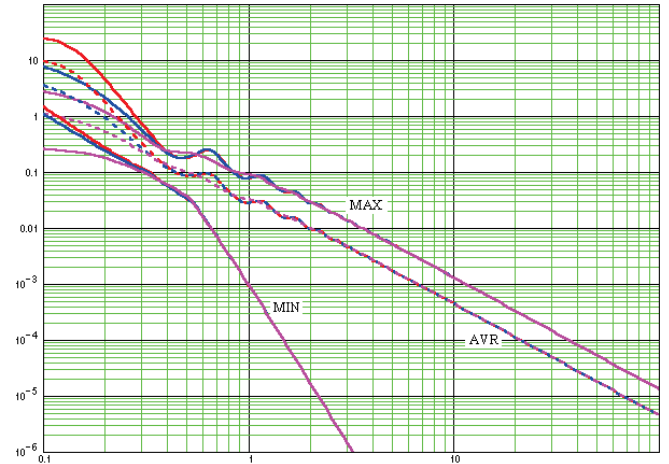


FIGURE 12. Maximum values (curves labeled “MAX”), average values (curves labeled “AVR”) and minimum values (curves labeled “MIN”) of the unnamed power gains for the three different setups defined for the arrangement of Fig. 11, as a function of D/λ .

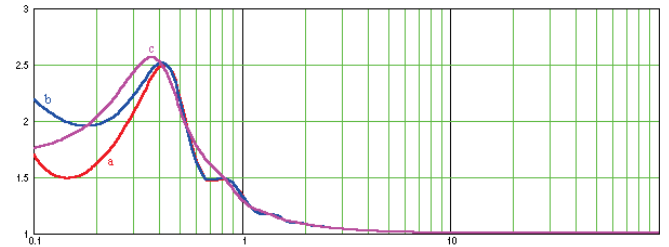


FIGURE 13. Rank measure of the unnamed power gain for the three different setups defined for the arrangement of Fig. 11, as a function of D/λ .

VI. SOME SIX-ANTENNA SETUPS

A. SIX PARALLEL ANTENNAS IN FREE SPACE

We consider an arrangement of six perfectly conducting parallel cylindrical center-fed dipole antennas lying in free space, forming two MAAs and shown in the not-to-scale drawing of Fig. 11. The total length of each antenna of MAA 1 is $l_1 = 0.94 \lambda/2$, and their spacing is $s = \lambda/4$. The total length of each antenna of MAA 2 is $l_2 = 0.94 \lambda/4$, and their spacing is s . All antennas have the same wire diameter $l_1/50$. The distance D between the MAAs is regarded as a variable. Four setups are defined as follows:

- in setup “a”, we assume that

$$\mathbf{Z}_{S1} = \begin{pmatrix} 0.05 - 16j & 0 & 0 \\ 0 & 0.05 - 16j & 0 \\ 0 & 0 & 0.05 - 16j \end{pmatrix} \Omega \quad (38)$$

and

$$\mathbf{Z}_{S2} = \begin{pmatrix} 1 + 20j & 0 & 0 \\ 0 & 1 + 20j & 0 \\ 0 & 0 & 1 + 20j \end{pmatrix} \Omega; \quad (39)$$

- in setup “b”, we assume that

$$\mathbf{Z}_{S1} = \begin{pmatrix} 3 & -1 - 2j & 1 + j \\ -1 - 2j & 2 + 3j & -2 - 2j \\ 1 + j & -2 - 2j & 3 - 2j \end{pmatrix} \Omega \quad (40)$$

and

$$\mathbf{Z}_{S2} = \begin{pmatrix} 4 + 25j & -1 - 3j & -2 - 2j \\ -1 - 3j & 5 + 12j & 1 + 5j \\ -2 - 2j & 1 + 5j & 6 + 27j \end{pmatrix} \Omega; \quad (41)$$

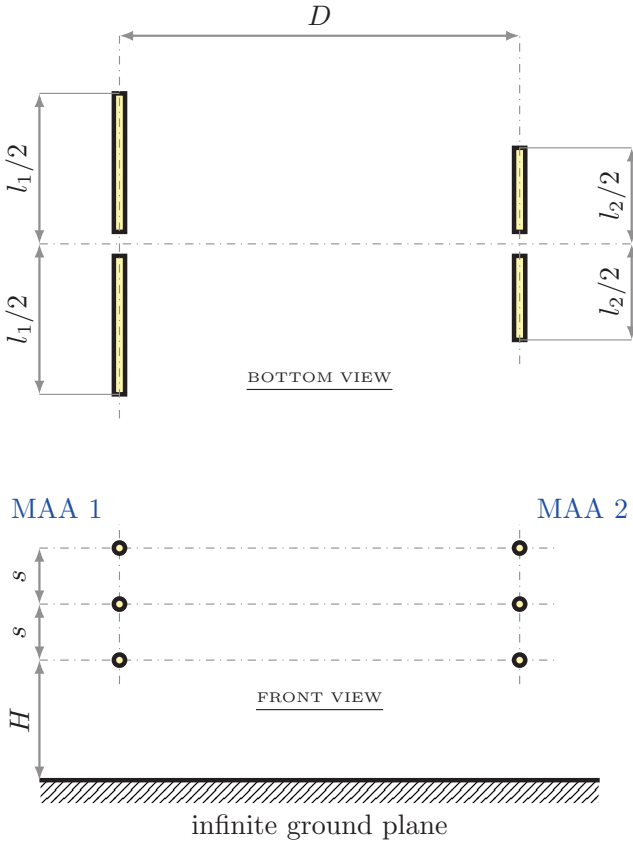


FIGURE 14. Six parallel antennas above a ground plane.

- in setup “c”, we assume that \mathbf{Z}_{S1} is 10 times the matrix given by (41) and \mathbf{Z}_{S2} is 10 times the matrix given by (40).

Each of these matrix is symmetric, and we checked that each of them has a positive definite hermitian part.

We have computed $G_{AU MAX}$, $G_{BU MAX}$, $G_{AU AVR}$, $G_{BU AVR}$, $G_{AU MIN}$ and $G_{BU MIN}$ as a function of D , for the three setups, using (17)–(20), (23)–(26) and the simulation technique summarized in Appendix C. We have checked that our results are compatible with (27)–(31).

Fig. 12 shows the quantities $G_{AU MAX} = G_{BU MAX}$, $G_{AU AVR} = G_{BU AVR}$ and $G_{AU MIN} = G_{BU MIN}$ for the different setups. According to the vanishing sensitivity to terminations for small coupling, we expect the three curves corresponding to each of these quantities to practically merge at a sufficient distance, and this is observed for $D \geq 2\lambda$. Most curves of Fig. 12 take on values that are greater than 1 at very short distances.

Fig. 13 shows $\rho_A = \rho_B$ for the different setups. The curves practically merge for $D \geq \lambda$. Furthermore, $\rho_A = \rho_B < 1.5$ for $D \geq 0.9\lambda$, and $\rho_A = \rho_B$ becomes very close to 1 for $D \geq 6\lambda$.

B. PARALLEL ANTENNAS ABOVE A GROUND PLANE

We now look at an arrangement of six perfectly conducting parallel cylindrical center-fed dipole antennas lying parallel to an infinite and perfectly conducting ground plane, forming

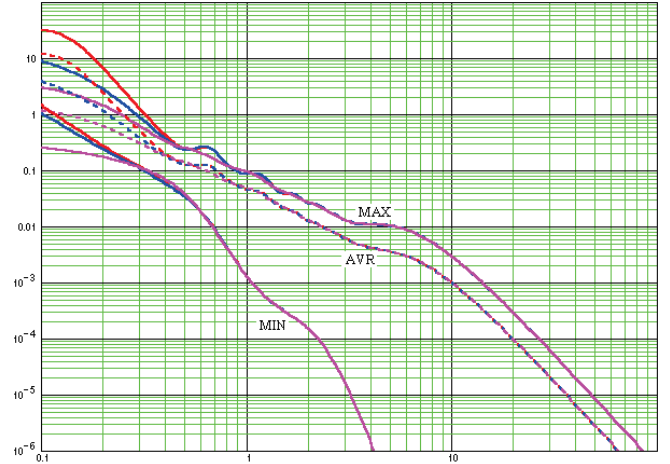


FIGURE 15. Maximum values (curves labeled “MAX”), average values (curves labeled “AVR”) and minimum values (curves labeled “MIN”) of the unnamed power gains for the three different setups defined for the arrangement of Fig. 14, and $H = \lambda$, as a function of D/λ .

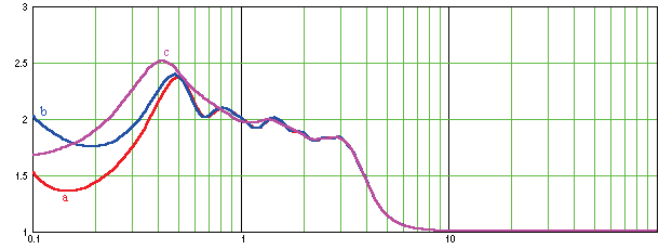


FIGURE 16. Rank measure of the unnamed power gain for the three setups defined for the arrangement of Fig. 14, and $H = \lambda$, as a function of D/λ .

two MAAs and shown in the not-to-scale drawing of Fig. 14. The antennas are identical to the ones used in Fig. 11. We use H to denote the height of both MAAs above the ground plane. Three different setups are defined as above for Fig. 11.

$G_{AU MAX}$, $G_{BU MAX}$, $G_{AU AVR}$, $G_{BU AVR}$, $G_{AU MIN}$ and $G_{BU MIN}$ were computed as above in Section VI.A. Fig. 15 and Fig. 16 show the maximum values, average values and minimum values of G_{AU} or G_{BU} , and $\rho_A = \rho_B$ for the different setups and $H = \lambda$. Fig. 17 and Fig. 18 show the same quantities for the different setups and $H = 10\lambda$. In Fig. 15 and Fig. 17, the vanishing sensitivity to terminations for small coupling is observed for $D \geq 2\lambda$. Most curves of Fig. 15 and Fig. 17 take on values that are greater than 1 at very short distances.

In Fig. 16 and Fig. 18, the curves practically merge for $D \geq 2\lambda$. In Fig. 16, $\rho_A = \rho_B < 1.5$ for $D \geq 4\lambda$, and $\rho_A = \rho_B$ becomes very close to 1 for $D \geq 7\lambda$. In Fig. 18, the region over which $\rho_A = \rho_B > 1.5$ is quite different from the corresponding regions of Fig. 13 and Fig. 16.

C. TEACHING OF THE NUMERICAL EXPERIMENTS

Our 2-MAA numerical experiments exemplify the vanishing sensitivity to terminations for small coupling, and show that the rank measure of the unnamed power gain $\rho_A = \rho_B$ effectively supplements the maximum values, average values and minimum values of G_{AU} or G_{BU} .

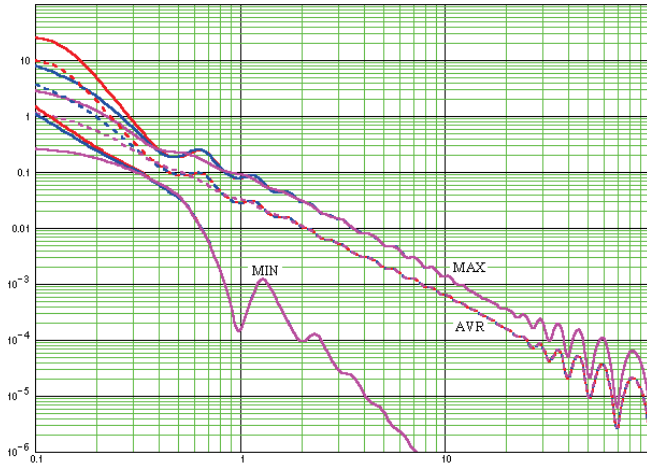


FIGURE 17. Maximum values (curves labeled “MAX”), average values (curves labeled “AVR”) and minimum values (curves labeled “MIN”) of the unnamed power gains for the three different setups defined for the arrangement of Fig. 14, and $H = 10\lambda$, as a function of D/λ .

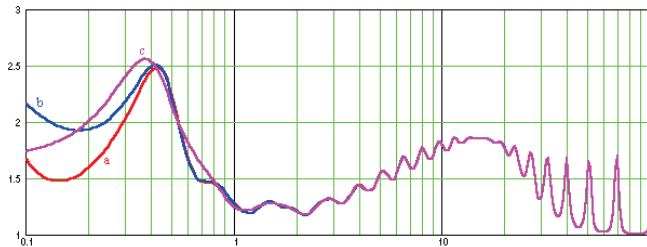


FIGURE 18. Rank measure of the unnamed power gain for the three setups defined for the arrangement of Fig. 14, and $H = 10\lambda$, as a function of D/λ .

VII. CONCLUSION

We have precisely defined and implemented two generalizations of the Friis transmission formula, which are collectively applicable to any number of reciprocal antennas, at any distance, in any reciprocal environment. These generalizations relate to the unnamed power gains of a radio link. They use the concepts of symmetry under link direction reversal, and of vanishing sensitivity to terminations for small coupling, which were introduced in Section II for the first generalization and in Section IV for the second generalization.

The other power gains studied in [7] and [8], namely the transducer power gains, the operating power gains, the available power gains, and the insertion power gains if $m = n$, do not have a property similar to the vanishing sensitivity to terminations for small coupling. In this sense, the vanishing sensitivity to terminations for small coupling is unique to the unnamed power gains.

In contrast, it is shown in [7] and [8] that if some conditions are met, the transducer power gains, and the insertion power gains if $m = n$, each have a property similar to the symmetry under link direction reversal. Accordingly, the symmetry under link direction reversal is not unique to the unnamed power gains.

We have also defined and investigated a new concept: the rank measure of the unnamed power gain, in a given direction. It is intended to better characterize the potential

of a radio link as regards spatial multiplexing or spatial diversity, because it is defined as the effective rank of a matrix that is closely related to the second generalization of the Friis transmission formula. We have shown that the rank measure of the unnamed power gain is invariant under link direction reversal, if some conditions are met.

A comparison between the results of the numerical experiments reported in Section III (where $\rho_A = \rho_B = 1$) and the ones reported in Section VI is instructive, and left to the reader.

APPENDIX A

This Appendix provides corrections to [7] and [8].

Several errors have been detected in [7]: in page 5, column 2, in the first sentence of Section IV.E, “operating power gains is” should be replaced with “operating power gain is”; in page 6, column 2, in the first sentence of Section V, “is lossless if and only if” should be replaced with “is lossless only if”; in page 6, column 2, in Section V, “ \mathbf{Z}_{APP2} ” should be replaced with “ \mathbf{Z}_{BPP2} ” (4 occurrences); in page 9, after equation (99), “where G_r is the effective area of the receiving antenna” should be replaced with “where G_r is the gain of the receiving antenna”; and in page 10, column 2, the titles of references [16] and [17] should be in italics instead of between quotation marks.

Note that in [7], in (79) the equality $G_{AT} = t_{A1}$ is not subject to the condition $P_{ARP1} \neq 0$ W, and in (80) the equality $G_{BT} = t_{B2}$ is not subject to the condition $P_{BRP2} \neq 0$ W. Thus, the presentation used in Section XI of [8] to introduce (320)–(322) is more general.

Several errors have been detected in [8]: in page 2, column 2, in the sentence following (4), “and the positive definite hermitian quadratic form $f_{\mathbf{D}} : \mathbb{C}^{\nu} \rightarrow \mathbb{R}$ such that $f_{\mathbf{D}}(\mathbf{x}) = \mathbf{x}^* \mathbf{D} \mathbf{x}$ ” should be replaced with “and the positive semidefinite hermitian quadratic form $f_{\mathbf{D}} : \mathbb{C}^{\nu} \rightarrow \mathbb{R}$ such that $f_{\mathbf{D}}(\mathbf{x}) = \mathbf{x}^* \mathbf{D} \mathbf{x}$ ”; in page 4, column 1, (17) should be replaced with

$$r(\mathbf{x}) = \frac{p_2(\mathbf{x})^* \mathbf{N} p_2(\mathbf{x})}{p_2(\mathbf{x})^* \mathbf{D} p_2(\mathbf{x})} = r(p_2(\mathbf{x})); \quad (42)$$

in page 12, column 2, at the end of Theorem 19, “if \mathbf{Y}_{SAM11} is invertible, for a specified DUS and a specified \mathbf{Z}_{S1} , G_{BOMIN} and G_{BOMAX} do not depend on \mathbf{Z}_{S2} ” should be replaced with “if \mathbf{Y}_{SAM22} is invertible, for a specified DUS and a specified \mathbf{Z}_{S1} , G_{BOMIN} and G_{BOMAX} do not depend on \mathbf{Z}_{S2} ”; in page 14, the first term of the right-hand side of (135) should be $\mathbf{I}_{S1}^* \mathbf{Z}_{PAM21}^* (\mathbf{Y}_{S2} + \mathbf{Y}_{S2}^*) \mathbf{Z}_{PAM21} \mathbf{I}_{S1}$ instead of $\mathbf{I}_{S1}^* \mathbf{Z}_{PAM21}^* (\mathbf{Y}_{S2} + \mathbf{Y}_{S2}) \mathbf{Z}_{PAM21} \mathbf{I}_{S1}$; in page 15, column 2, a full stop is missing after “are positive semidefinite”; in page 33, column 2, after (359), “because \mathbf{Z} is the impedance matrix of a lossless DUT” should be replaced with “because \mathbf{Z} is the impedance matrix of a lossless DUS”; in page 34, column 1, “of Theorem 29 on unnamed power gain in CA and CB” should be replaced with “of Theorem 29 on unnamed power gains in CA and CB”; and, throughout the article, “right hand side” should be replaced with “right-hand side” (1 occurrence) and “right hand sides” with “right-hand sides” (4 occurrences).

Note that, in Appendix C of [8], the proof of (372) uses the assumption that $\mathbf{V}_{O1}^* \mathbf{Y}_{N1} \mathbf{V}_{O1}$ and $\mathbf{I}_{S1}^* \mathbf{Z}_{N1} \mathbf{I}_{S1}$ are the same power for any excitation, and that $\mathbf{V}_{O1}^* \mathbf{Y}_{D1} \mathbf{V}_{O1}$ and $\mathbf{I}_{S1}^* \mathbf{Z}_{D1} \mathbf{I}_{S1}$ are the same power for any excitation. This assumption was satisfied wherever (372) was used in [8].

Likewise, in Appendix C of [8], the proof of (373) uses the assumption that $\mathbf{V}_{O2}^* \mathbf{Y}_{N2} \mathbf{V}_{O2}$ and $\mathbf{I}_{S2}^* \mathbf{Z}_{N2} \mathbf{I}_{S2}$ are the same power for any excitation, and that $\mathbf{V}_{O2}^* \mathbf{Y}_{D2} \mathbf{V}_{O2}$ and $\mathbf{I}_{S2}^* \mathbf{Z}_{D2} \mathbf{I}_{S2}$ are the same power for any excitation. This assumption was satisfied wherever (373) was used in [8].

APPENDIX B

In this Appendix B, we establish some additional formulas about Y_{AAVP2} , Y_{ARP1} , Y_{BAVP1} and Y_{BRP2} , using the notations and assumptions of Section II. We write

$$\mathbf{Z} = \begin{pmatrix} Z_{11} & Z_{12} \\ Z_{21} & Z_{22} \end{pmatrix}. \quad (43)$$

The DUS being passive, $H(\mathbf{Z})$ is positive semidefinite. By [13, Sec. 7.1.2], we consequently have $\text{Re}(Z_{11}) \geq 0$. Since $\text{Re}(Z_{S1}) > 0$, it follows that $Z_{11} + Z_{S1} \neq 0$. Likewise, we get $Z_{22} + Z_{S2} \neq 0$. Accordingly, we easily show that the generator connected to port 1 in CA sees an impedance

$$Z_{APP1} = Z_{11} - \frac{Z_{12}Z_{21}}{Z_{22} + Z_{S2}}, \quad (44)$$

and the generator connected to port 2 in CB sees an impedance

$$Z_{APP2} = Z_{22} - \frac{Z_{12}Z_{21}}{Z_{11} + Z_{S1}}. \quad (45)$$

It follows from (4) and (5) that

$$\mathbf{Y}_{SAM} = \frac{1}{\Delta} \begin{pmatrix} Z_{22} + Z_{S2} & -Z_{12} \\ -Z_{21} & Z_{11} + Z_{S1} \end{pmatrix}, \quad (46)$$

where

$$\Delta = (Z_{11} + Z_{S1})(Z_{22} + Z_{S2}) - Z_{12}Z_{21}. \quad (47)$$

Using (44)–(47) in (8)–(11), we obtain

$$Y_{AAVP2} = \frac{|Z_{21}|^2}{4|Z_{11} + Z_{S1}|^2 \text{Re}(Z_{APP2})}, \quad (48)$$

$$Y_{ARP1} = \frac{\text{Re}(Z_{APP1})}{|Z_{APP1} + Z_{S1}|^2}, \quad (49)$$

$$Y_{BAVP1} = \frac{|Z_{12}|^2}{4|Z_{22} + Z_{S2}|^2 \text{Re}(Z_{APP1})} \quad (50)$$

and

$$Y_{BRP2} = \frac{\text{Re}(Z_{APP2})}{|Z_{APP2} + Z_{S2}|^2}. \quad (51)$$

It follows that

$$G_{AU} = \frac{|Z_{21}|^2 |Z_{APP1} + Z_{S1}|^2}{4|Z_{11} + Z_{S1}|^2 \text{Re}(Z_{APP1}) \text{Re}(Z_{APP2})} \quad (52)$$

and

$$G_{BU} = \frac{|Z_{12}|^2 |Z_{APP2} + Z_{S2}|^2}{4|Z_{22} + Z_{S2}|^2 \text{Re}(Z_{APP1}) \text{Re}(Z_{APP2})}. \quad (53)$$

APPENDIX C

This Appendix C provides a short explanation about the simulation results presented in this work.

The center-fed cylindrical dipole antennas are excited by a delta-gap source when they are used for emission. The simulation are obtained using a method-of-moment-based program implementing the computation technique presented in [15, Ch. 2]. According to this approach, we solve Hallén integral equation, and the numerical solutions are obtained using Lagrange polynomials of order 2 for the basis functions, and point-matching.

Between points belonging to the same dipole antenna, we implement an accurate approximation of the exact thin-wire kernel proposed in [16, Sec. 24.7]. A part of the kernel, comprising all ill-behaved terms, is integrated exactly using known primitives, the other terms of the kernel are integrated numerically. Between points belonging to different dipole antennas, we implement the same approximate thin-wire kernel as the one used in [15, Ch. 2].

When an infinite ground plane is present, we assume that it is perfectly conducting, and it is taken into account using image theory.

This computation provides an impedance matrix, of size 2 by 2 for two antennas, or of size $m + n$ by $m + n$ for two MAAs. This matrix is close to a symmetric matrix. However, to enforce an exact reciprocity, the symmetric part of this matrix is assumed to be equal to \mathbf{Z} .

APPENDIX D

In this Appendix D, we establish some additional formulas about \mathbf{Y}_{AAVP2} , \mathbf{Y}_{ARP1} , \mathbf{Y}_{BAVP1} and \mathbf{Y}_{BRP2} , using the notations of Section IV.

The matrix \mathbf{Z} is of size $(m + n)$ by $(m + n)$ and it may be partitioned into four submatrices, \mathbf{Z}_{11} of size m by m , \mathbf{Z}_{12} of size m by n , \mathbf{Z}_{21} of size n by m and \mathbf{Z}_{22} of size n by n , which are such that

$$\mathbf{Z} = \begin{pmatrix} \mathbf{Z}_{11} & \mathbf{Z}_{12} \\ \mathbf{Z}_{21} & \mathbf{Z}_{22} \end{pmatrix}. \quad (54)$$

The DUS being passive, $H(\mathbf{Z})$ is positive semidefinite. By [13, Sec. 7.1.2], \mathbf{Z}_{11} is such that $H(\mathbf{Z}_{11})$ is positive semidefinite. Since $H(\mathbf{Z}_{S1})$ is positive definite, it follows that $H(\mathbf{Z}_{11} + \mathbf{Z}_{S1})$ is positive definite. By Lemma 1 of [11], it follows that $\mathbf{Z}_{11} + \mathbf{Z}_{S1}$ is invertible. Likewise, $\mathbf{Z}_{22} + \mathbf{Z}_{S2}$ is invertible. Accordingly, we easily show that the generator connected to port set 1 in CA sees an impedance matrix

$$\mathbf{Z}_{APP1} = \mathbf{Z}_{11} - \mathbf{Z}_{12}(\mathbf{Z}_{22} + \mathbf{Z}_{S2})^{-1} \mathbf{Z}_{21} \quad (55)$$

and the generator connected to port set 2 in CB sees an impedance matrix

$$\mathbf{Z}_{APP2} = \mathbf{Z}_{22} - \mathbf{Z}_{21}(\mathbf{Z}_{11} + \mathbf{Z}_{S1})^{-1} \mathbf{Z}_{12}. \quad (56)$$

\mathbf{Z}_{APP1} being the impedance matrix of a passive system, it must be such that $H(\mathbf{Z}_{APP1})$ is positive semidefinite. Since $H(\mathbf{Z}_{S1})$ is positive definite, it follows that $H(\mathbf{Z}_{APP1} + \mathbf{Z}_{S1})$ is positive definite. By Lemma 1 of [11], it follows that

$$\mathbf{G}_{AU} = \frac{\mathbf{V}_{O1}^*(\mathbf{Z}_{S1} + \mathbf{Z}_{11})^{-1*} \mathbf{Z}_{21}^* H(\mathbf{Z}_{APP2})^{-1} \mathbf{Z}_{21} (\mathbf{Z}_{S1} + \mathbf{Z}_{11})^{-1} \mathbf{V}_{O1}}{4 \mathbf{V}_{O1}^* (\mathbf{Z}_{S1} + \mathbf{Z}_{APP1})^{-1*} H(\mathbf{Z}_{APP1}) (\mathbf{Z}_{S1} + \mathbf{Z}_{APP1})^{-1} \mathbf{V}_{O1}} \quad (65)$$

and

$$\mathbf{G}_{BU} = \frac{\mathbf{V}_{O2}^*(\mathbf{Z}_{S2} + \mathbf{Z}_{22})^{-1*} \mathbf{Z}_{12}^* H(\mathbf{Z}_{APP1})^{-1} \mathbf{Z}_{12} (\mathbf{Z}_{S2} + \mathbf{Z}_{22})^{-1} \mathbf{V}_{O2}}{4 \mathbf{V}_{O2}^* (\mathbf{Z}_{S2} + \mathbf{Z}_{APP2})^{-1*} H(\mathbf{Z}_{APP2}) (\mathbf{Z}_{S2} + \mathbf{Z}_{APP2})^{-1} \mathbf{V}_{O2}}. \quad (66)$$

$\mathbf{Z}_{APP1} + \mathbf{Z}_{S1}$ is invertible. Likewise, $\mathbf{Z}_{APP2} + \mathbf{Z}_{S2}$ is invertible.

It follows from the formula for the inverse of a partitioned matrix [13, Sec. 0.7.3], [14, Sec. 0.7.3] that

$$\mathbf{Y}_{SAM11} = (\mathbf{Z}_{S1} + \mathbf{Z}_{APP1})^{-1}, \quad (57)$$

$$\begin{aligned} \mathbf{Y}_{SAM12} &= -(\mathbf{Z}_{S1} + \mathbf{Z}_{11})^{-1} \mathbf{Z}_{12} (\mathbf{Z}_{S2} + \mathbf{Z}_{APP2})^{-1} \\ &= -(\mathbf{Z}_{S1} + \mathbf{Z}_{APP1})^{-1} \mathbf{Z}_{12} (\mathbf{Z}_{S2} + \mathbf{Z}_{22})^{-1}, \end{aligned} \quad (58)$$

$$\begin{aligned} \mathbf{Y}_{SAM21} &= -(\mathbf{Z}_{S2} + \mathbf{Z}_{APP2})^{-1} \mathbf{Z}_{21} (\mathbf{Z}_{S1} + \mathbf{Z}_{11})^{-1} \\ &= -(\mathbf{Z}_{S2} + \mathbf{Z}_{22})^{-1} \mathbf{Z}_{21} (\mathbf{Z}_{S1} + \mathbf{Z}_{APP1})^{-1} \end{aligned} \quad (59)$$

and

$$\mathbf{Y}_{SAM22} = (\mathbf{Z}_{S2} + \mathbf{Z}_{APP2})^{-1}. \quad (60)$$

In Section IV, we assume that $H(\mathbf{Y}_{SAM11}^{-1} - \mathbf{Z}_{S1})$ and $H(\mathbf{Y}_{SAM22}^{-1} - \mathbf{Z}_{S2})$ are invertible. It follows that $H(\mathbf{Z}_{APP1})$ and $H(\mathbf{Z}_{APP2})$ are invertible.

Using (57)–(60) in (17)–(20), we obtain

$$\begin{aligned} \mathbf{Y}_{AAVP2} &= \frac{1}{4} (\mathbf{Z}_{S1} + \mathbf{Z}_{11})^{-1*} \mathbf{Z}_{21}^* \\ &\quad \times H(\mathbf{Z}_{APP2})^{-1} \mathbf{Z}_{21} (\mathbf{Z}_{S1} + \mathbf{Z}_{11})^{-1}, \end{aligned} \quad (61)$$

$$\begin{aligned} \mathbf{Y}_{ARP1} &= (\mathbf{Z}_{S1} + \mathbf{Z}_{APP1})^{-1*} \\ &\quad \times H(\mathbf{Z}_{APP1}) (\mathbf{Z}_{S1} + \mathbf{Z}_{APP1})^{-1}, \end{aligned} \quad (62)$$

$$\begin{aligned} \mathbf{Y}_{BAVP1} &= \frac{1}{4} (\mathbf{Z}_{S2} + \mathbf{Z}_{22})^{-1*} \mathbf{Z}_{12}^* \\ &\quad \times H(\mathbf{Z}_{APP1})^{-1} \mathbf{Z}_{12} (\mathbf{Z}_{S2} + \mathbf{Z}_{22})^{-1} \end{aligned} \quad (63)$$

and

$$\begin{aligned} \mathbf{Y}_{BRP2} &= (\mathbf{Z}_{S2} + \mathbf{Z}_{APP2})^{-1*} \\ &\quad \times H(\mathbf{Z}_{APP2}) (\mathbf{Z}_{S2} + \mathbf{Z}_{APP2})^{-1}. \end{aligned} \quad (64)$$

Thus, \mathbf{G}_{AU} and \mathbf{G}_{BU} are given by (65) and (66) shown at the top of this page.

ACKNOWLEDGMENTS

This work was supported by the Czech Science Foundation under project No. 21-19025M. This material is based on work supported by the National Science Foundation under Grant No. 2030165.

REFERENCES

- [1] H.T. Friis, "A note on a simple transmission formula," *Proceedings of the I.R.E. and Waves and Electrons*, vol. 34, no. 5, pp. 254-256, May 1946.
- [2] F.E. Terman, *Electronic and Radio Engineering*, 4th ed., International Student Edition, New York, NY, USA: McGraw-Hill, 1955.
- [3] H. Baudrand, "On the generalizations of the maximum power transfer theorem", *Proc. IEEE*, vol. 58, no. 10, pp. 1780-1781, Oct. 1970.
- [4] *IEEE Standard for Definitions of Terms for Antennas*, IEEE Std 145-2013, Mar. 2014.
- [5] W.L. Stutzman, G.A. Thiele, *Antenna Theory and Design*, Third Edition, Hoboken, NJ, USA: John Wiley & Sons, 2013.
- [6] H.T. Friis, "Introduction to radio and radio antennas," *IEEE Spectrum*, vol. 8, no. 4, pp. 55-61, Apr. 1971.
- [7] F. Broyd  and E. Clavelier, "About the Power Ratios Relevant to a Passive Linear Time-Invariant 2-Port," *Excem Research Papers in Electronics and Electromagnetics*, no. 5, doi: 10.5281/zenodo.6555682, May 2022.
- [8] F. Broyd  and E. Clavelier, "Some Results on Power in Passive Linear Time-Invariant Multiports, Part 3," *Excem Research Papers in Electronics and Electromagnetics*, no. 7, doi: 10.5281/zenodo.8124511, Jul. 2023.
- [9] E.C. Jordan and K.G. Balmain, *Electromagnetic Waves and Radiating Systems*, 2nd ed., Englewood Cliffs, NJ, USA: Prentice-Hall, 1968.
- [10] J.R. Carson, "Reciprocal theorems in radio communication," *Proceedings of the Institute of Radio Engineers*, vol. 17, no. 6, pp. 952-956, Jun. 1929.
- [11] F. Broyd  and E. Clavelier, "Some Results on Power in Passive Linear Time-Invariant Multiports, Part 1," *Excem Research Papers in Electronics and Electromagnetics*, no. 2, doi: 10.5281/zenodo.4419637, Jan. 2021.
- [12] O. Roy and M. Vitterli, "The effective rank: a measure of effective dimensionality," *Proc. 15th European Signal Processing Conference, EUSIPCO 2007*, pp. 606-610, Sept. 2007.
- [13] R.A. Horn and C.R. Johnson, *Matrix analysis*, 2nd ed., New York, NY, USA: Cambridge University Press, 2013.
- [14] R.A. Horn and C.R. Johnson, *Matrix analysis*, New York, NY, USA: Cambridge University Press, 1985.
- [15] R.E. Collin, *Antennas and Radiowave Propagation*, International Edition, New York, NY, USA: McGraw-Hill, 1985.
- [16] S.J. Orfanidis, *Electromagnetic Waves and Antennas — vol. 2 — Antennas*, Sophocles J. Orfanidis, 2016.



FR D RIC BROYD  was born in France in 1960. He received the M.S. degree in physics engineering from the Ecole Nationale Sup rieure d'Ing nieurs Electriciens de Grenoble (ENSIEG) and the Ph.D. in microwaves and microtechnologies from the Universit  des Sciences et Technologies de Lille (USTL).

He co-founded the Excem corporation in May 1988, a company providing engineering and research and development services. He is president of Excem since 1988. He is now also president and CTO of Eurexcem, a subsidiary of Excem. Most of his activity is allocated to engineering and research in electronics, radio, antennas, electromagnetic compatibility (EMC) and signal integrity.

Dr. Broyd  is author or co-author of about 100 technical papers, and inventor or co-inventor of about 90 patent families, for which 73 patents of France and 49 patents of the USA have been granted. He is a Senior Member of the IEEE since 2001. He is a licensed radio amateur (F5OYE).



EVELYNE CLAVELIER was born in France in 1961. She received the M.S. degree in physics engineering from the Ecole Nationale Supérieure d'Ingénieurs Electriciens de Grenoble (ENSIEG).

She is co-founder of the Excem corporation, based in Maule, France, and she is currently CEO of Excem. She is also president of Tekcem, a company selling or licensing intellectual property rights to foster research. She is an active engineer and researcher.

Her current research areas are radio communications, antennas, matching networks, EMC and circuit theory.

Prior to starting Excem in 1988, she worked for Schneider Electric (in Grenoble, France), STMicroelectronics (in Grenoble, France), and Signetics (in Mountain View, CA, USA).

Ms. Clavelier is the author or a co-author of about 90 technical papers. She is co-inventor of about 90 patent families. She is a Senior Member of the IEEE since 2002. She is a licensed radio amateur (F1PHQ).



LUKÁS JELINEK received his Ph.D. degree from the Czech Technical University in Prague, Czech Republic, in 2006. In 2015, he was appointed Associate Professor at the Department of Electromagnetic Field at the same university.

Since 2006, he is also head of the National Reference Laboratory for Non-Ionizing Radiation at The National Institute of Public Health of the Czech Republic.

His research interests include wave propagation in complex media, electromagnetic field theory, metamaterials, numerical techniques and optimization.



MILOSLAV CAPEK received the M.Sc. degree in Electrical Engineering 2009, the Ph.D. degree in 2014, and was appointed Full Professor in 2023, all from the Czech Technical University in Prague, Czech Republic.

He leads the development of the AToM (Antenna Toolbox for Matlab) package. His research interests include electromagnetic theory, electrically small antennas, antenna design, numerical techniques, and optimization. He authored or co-authored over 150 journal and conference papers.

Dr. Capek is a Senior Member of the IEEE since 2017. He is Associate Editor of IET Microwaves, Antennas & Propagation. He was a regional delegate of EurAAP between 2015 and 2020 and an associate editor of Radioengineering between 2015 and 2018. He received the IEEE Antennas and Propagation Edward E. Altshuler Prize Paper Award 2023.



KARL F. WARNICK received the BS degree in Electrical Engineering and Mathematics and the PhD degree in Electrical Engineering from Brigham Young University (BYU), Provo, UT, in 1994 and 1997, respectively.

From 1998 to 2000, he was a Postdoctoral Research Associate and Visiting Assistant Professor in the Center for Computational Electromagnetics at the University of Illinois at Urbana-Champaign.

Since 2000, he has been a faculty member in the Department of Electrical and Computer Engineering at BYU, where he is currently a Professor.

Dr. Warnick is a Fellow of the IEEE since 2013. He has published many books, scientific articles, and conference papers on electromagnetic theory, numerical methods, antenna applications, and high sensitivity phased arrays for satellite communications and radio astronomy.

•••